applied sciences

MDPI

Article

Failure Probability Analysis of the Transmission Line Considering Uncertainty Under Combined Ice and Wind Loads

Jiaxiang Li [1], Chao Zhang [1], Jian Zhang [2,*], Xuesheng Zhang [3] and Wenrui Wang [1]

[1] School of Resources and Civil Engineering, Northeastern University, Shenyang 110819, China; lijx@mail.neu.edu.cn (J.L.); zhangchao_neu@126.com (C.Z.); wangwrwy@163.com (W.W.)
[2] China Power Engineering Consulting Group, Northeast Electric Power Design Institute Co., Ltd., Changchun 130022, China
[3] Beijing Urban Construction Group Co., Ltd., Beijing 100088, China; zxswwy0927@163.com
* Correspondence: zhangjian_2022@yeah.net

Abstract: The probability of accidents, including conductor breakage and tower collapse, for the transmission tower-line system significantly increases under combined ice and wind loads. The existing research on the failure probability of the tower-line system under combined ice and wind loads is limited to static calculation, ignoring the fluctuating effect of wind. In addition, uncertainty in the material strength and geometric dimensions of the structure due to the production process and other pertinent factors could affect the bearing capacity of the tower. To accurately assess the failure probability of transmission lines under combined ice and wind loads, this paper first established numerical models of the transmission tower-line system considering structural uncertainty based on the Latin Hypercube Sampling method. And then, the limit performance indexes of the uncertain models were determined by Pushover analysis. Subsequently, considering the joint probability distributions of ice thickness–wind speed and wind speed–wind direction, the failure probability of the tower-line system under ice and wind loads was calculated. Finally, the influence of structural uncertainty and fluctuating wind on the failure probability was discussed. The results showed that, compared with structural uncertainty, the fluctuating effect of wind had a more significant influence on the failure probability of the tower-line system under combined ice and wind loads. After considering the fluctuating effect of wind, the smaller ice loads can potentially lead to the failure of the transmission tower-line system.

Keywords: failure probability; ice and wind loads; uncertainty analysis; dynamic analysis; transmission tower-line system

Citation: Li, J.; Zhang, C.; Zhang, J.; Zhang, X.; Wang, W. Failure Probability Analysis of the Transmission Line Considering Uncertainty Under Combined Ice and Wind Loads. *Appl. Sci.* **2024**, *14*, 10752. https://doi.org/10.3390/app142210752

Academic Editor: Giuseppe Lacidogna

Received: 7 October 2024
Revised: 18 November 2024
Accepted: 19 November 2024
Published: 20 November 2024

1. Introduction

Previous ice disasters have illustrated that ice can cause electrical issues, including short circuits on transmission lines, and mechanical failures such as conductor breakage or even tower collapse, posing a significant threat to the stable operation of the electrical power system [1–3]. To prevent the damage of transmission lines during ice disasters, scholars have conducted extensive research on predicting ice loads and analyzing the mechanical response of transmission tower-line systems under icing conditions. Based on field measurement data, Jiang et al. [4] proposed a correction coefficient to enhance the accuracy of uneven icing assessment on transmission lines. Zhang et al. [5,6] investigated the growth mechanism of ice on transmission lines and introduced a novel median volume diameter of the droplet distribution, which was derived from microscopic meteorological data and utilized for calculating the collision coefficient. Yang et al. [7] proposed a method to calculate the equivalent ice thickness of transmission lines based on conductor tension by establishing the state equations of the conductor. Li et al. [8,9] studied the mechanical response of a tower-line system subjected to ice shedding and conductor breakage.

In the aforementioned studies, the researchers investigated the ice loads on transmission lines from a microscopic perspective and analyzed the specific mechanical responses of the transmission lines. However, the relationship between ice load and the failure probability of transmission lines from a macroscopic perspective has not been fully explored. There is a lack of assessment on the failure probability of transmission tower-line systems under varying ice loads. Regarding probabilistic approaches, Lehner et al. [10] and Brozovsky et al. [11] adopted the approach based on the traditional Wöhler concept and the direct optimized probabilistic computation method to study the influence of fatigue damage on the steel support truss during the whole service life, respectively. Ferrari et al. [12] used the two structural limit analysis algorithms they previously proposed [13,14] to predict the elastoplastic response of the infrastructure to evaluate the collapse state of the truss-frame structure. Subsequently, Cocchetti et al. extended the spirit of these algorithms to spatial cable-rib structures, and proposed a complementarity problem formulation for simulating the mechanical behavior of cable-rib structures [15,16]. In addition, fragility analysis is another primary method for calculating the failure probability of structures, which can evaluate the bearing capacity of the structure from a probabilistic perspective [17,18]. Zhu et al. [19] conducted an incremental dynamic analysis (IDA) on a specific transmission tower project under different wind attack angles, determined the fragility curve of the tower, and evaluated the failure probability of the tower. The results showed that the most unfavorable wind attack angle for this engineering case was 45°. Tian et al. [20] investigated the dynamic response of transmission towers subjected to near-field earthquakes, constructed an earthquake probability model utilizing the IDA method, and studied the influence of seismic incident angle on structural fragility. Dikshit and Alipour [21] proposed a moment-matching method for calculating the vulnerability of transmission towers under wind loads through wind tunnel tests and nonlinear buckling analysis.

The above studies on the fragility of transmission lines focused on single loads, yet the influence of wind load during ice disasters cannot be ignored. In addition, ice on transmission lines also increases the windward area of the structure, resulting in an increased wind load. Therefore, both ice and wind loads should be considered simultaneously for the analysis of icing transmission lines. A fragility analysis of the structure under combined ice and wind loads should be conducted [22]. Li et al. [23] proposed a life safety assessment method by calculating the fragility under combined wind and earthquake loads, which can calculate the collapse probability of the tower under different wind loads. Xiao et al. [24] introduced a fragility surface for assessing a transmission tower-line system under combined ice and wind loads, and analyzed the effects of wind direction and material properties on fragility. The results indicated that wind direction had a significant impact on the bearing capacity of the tower-line system. Mahmoudi et al. [25] analyzed the meteorological parameters in the region where a 400 Kv transmission line was located, studying the interactions between maximum wind speed, maximum ice thickness, and temperature, and calculated the fragility curve of the transmission line under different combined ice and wind loads.

Although the fragility analysis method can evaluate the failure probability of transmission lines under different combined ice and wind loads, the studies mentioned above ignored the randomness and occurrence probabilities of ice loads and wind loads [26]. Therefore, to more accurately assess the failure probability of tower-line systems under combined ice and wind loads, it is necessary to consider the joint probability distribution between ice loads and wind loads. The Copula function joint distribution theory, which considers the correlation between variables, is widely used for constructing multivariate joint probability distributions [27]. Yang et al. [28] employed the Copula function to develop a joint probability distribution of ice thickness and wind speed, and predicted the failure probability of transmission lines utilizing the extreme learning machine method, but ignored the correlation between wind speed and wind direction. Li et al. [29] established joint probability distributions of ice thickness and wind speed, wind speed and wind direction through Copula function. Subsequently, they combined these distributions with the fragility analysis method to propose a failure probability analysis approach that considers

the joint probability of ice and wind loads, and assessed the failure probability of the tower-line system. Nonetheless, their work utilized the static analysis method, neglecting the fluctuating nature of wind. The natural wind speed is composed of mean wind speed and fluctuating wind speed. The mean wind speed remains relatively constant and can be considered a static load. However, the fluctuating wind speed varies continuously over time, thereby inducing dynamic responses of the structures. Existing studies have indicated that the fluctuating effect of wind can lead to significant variations in the mechanical response of structures [30]. Therefore, it is necessary to conduct a dynamic analysis of the tower-line system under combined ice and wind loads considering the fluctuating effect of wind load.

The aforementioned studies on the failure probability of transmission lines under combined ice and wind loads have employed certain models, in which the material parameters and geometric dimensions of the structure are treated as constant. However, during the processes of material manufacturing, transportation, and installation of structural components, there may be deviations in the material strength and geometric dimensions from the designed values [31,32]. Fu et al. [33–35] established uncertain finite element models (FEMs) of the transmission tower-line system using the Latin Hypercube Sampling method (LHS), and analyzed the vulnerability of transmission tower under wind loads. The results showed that the influence of material uncertainty on fragility is more significant than that of geometric uncertainty. Tian and Liu [36] studied the influence of the structural uncertainty on the dynamic response of the transmission tower subjected to conductor breakage. The results showed that the yield strength of the diagonal member and the geometric size of the member had a significant effect on the results. Fu et al. [37] studied the seismic response of uncertain transmission lines by combining LHS and IDA methods. The results showed that the influence of structural parameter uncertainty should be considered when assessing the seismic performance of transmission tower-line system. Ma et al. [38] considered the probability distribution of ice and wind speed, and introduced the uncertainty of structural parameters to analyze the failure probability of American pine power poles under combined ice and wind loads. However, in this study, ice load and wind load were assumed to be independent variables, and the correlation between the two environmental factors was not considered. In addition, the probability of the wind direction and the fluctuating effect of wind were ignored.

A comprehensive review of the above-mentioned works indicates that there is currently limited research on the failure probability of transmission lines under combined ice and wind loads, considering the uncertainties of structural parameters and the fluctuating effect of the wind. Therefore, to accurately evaluate the failure probability of transmission lines under combined ice and wind loads, based on Li et al.'s studies [29,39], this paper established the uncertain transmission tower-line system models using the LHS method, and then considering the fluctuating effect of wind, a fragility analysis of transmission lines under combined ice and wind loads was conducted. Finally, the failure probability of the tower-line system was calculated based on joint probability distribution models of ice thickness–wind speed (IT–WS) and wind speed–wind direction (WS–WD). In Sections 2 and 3, the failure probability analysis and the uncertain FEMs of transmission tower-line systems are introduced, respectively. In Section 4, the limit performance index for the tower-line system is determined. In Section 5, the failure probability of the transmission tower-line system under combined ice and wind loads is calculated and the influences of the uncertain parameters and fluctuating wind are discussed. Section 6 concludes the study.

2. Failure Probability Analysis

2.1. Method

Fragility analysis can be used to calculate the failure probability of structures in the case of single disasters or double disasters. However, when calculating the failure probability of the structure under double disasters, the fragility analysis ignores the correlation between

the two disasters. Therefore, based on the joint probability distribution of WS–WD and IT–WS, this paper calculates the failure probability of transmission lines under combined ice and wind loads. Equations (1) and (2), respectively, give the calculation formulas of the failure probability density and the cumulative failure probability of the transmission line under combined ice and wind loads [29]:

$$P_\varphi = F_\varphi(im_1, im_2) \cdot f_{IM_1,IM_2}(im_1, im_2) \cdot P(\varphi | im_{21}, im_{22}) \tag{1}$$

$$T_\varphi = \int_{im_{21}}^{im_{22}} \int_{im_{11}}^{im_{12}} F_\varphi(im_1, im_2) \cdot f_{IM_1,IM_2}(im_1, im_2) \cdot P(\varphi | im_{21}, im_{22}) dim_1 dim_2 \tag{2}$$

where P_φ and T_φ are the failure probability density and the cumulative failure probability, respectively; im_1 and im_2 are the ice thickness and wind speed; $F_\varphi(im_1, im_2)$ is the fragility function of tower-line system under combined ice and wind loads at wind direction φ; $f_{IM_1,IM_2}(im_1, im_2)$ is the joint probability distribution of IT–WS; $P(\varphi | im_{21}, im_{22})$ is the probability of wind direction φ in the $im_{21} - im_{22}$ wind speed range.

2.2. Joint Probability Distribution Model of Ice and Wind Loads

In this paper, data on ice, wind speed, and wind direction from 1973 to 2020 for the cities of Chenzhou, Yongzhou, and Shaoyang in Hunan Province, China, are collected through the National Oceanic and Aeronautic Administration (NOAA) website. Based on the Akaike Information Criterion (AIC) and the Bayesian Information Criterion (BIC), the joint probability distribution models of IT–WS and WS–WD are established using the Clayton Copula function (Equation (3)) and Frank Copula function (Equation (4)), respectively. Figure 1 shows the joint probability density of IT–WS and WS–WD. More details on the construction of the joint probability distribution model can be found in Li et al.'s study [29].

$$F_{XY} = C_1(u_1, v_1, \theta_1) = \left(u_1^{-\theta_1} + v_1^{-\theta_1} - 1\right)^{-1/\theta_1} \tag{3}$$

$$P_{XY} = C_2(u_2, v_2, \theta_2) = -\frac{1}{\theta_2} \ln\left[1 + \frac{\left(e^{-\theta_2 u_2} - 1\right)\left(e^{-\theta_2 v_2} - 1\right)}{e^{-\theta_2} - 1}\right] \tag{4}$$

where F_{XY} is the Clayton Copula joint probability distribution model; u_1 and v_1 are ice thickness and wind speed cumulative probability density functions; P_{XY} is the Frank Copula joint probability distribution model; u_2 and v_2 are wind speed and wind direction cumulative probability density functions; θ_1 and θ_2 are the parameters of the Copula function.

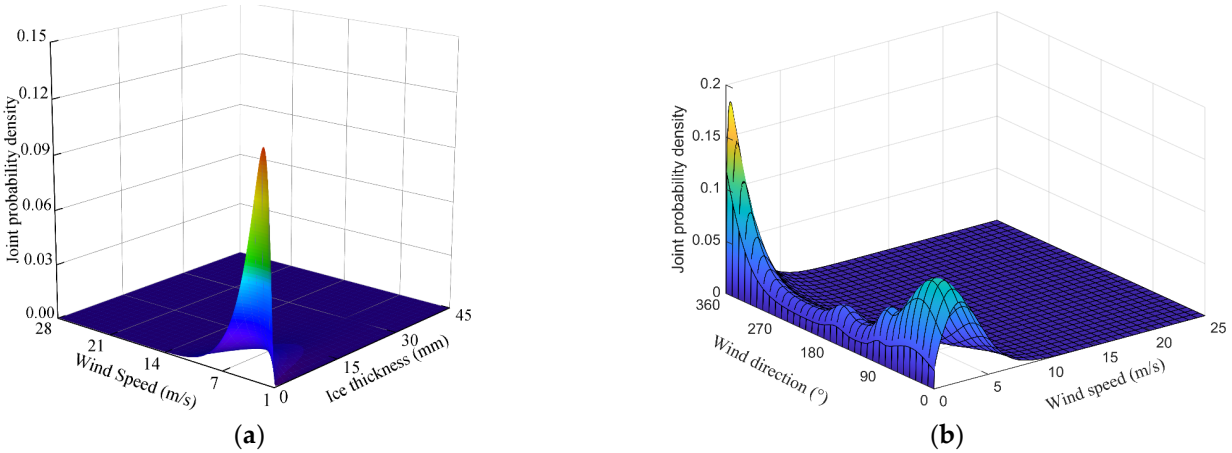

Figure 1. The joint probability density distribution: (**a**) IT–WS; (**b**) WS–WD.

2.3. Fragility Function

To calculate the failure probability of the tower-line system under combined ice and wind loads, it is necessary to analyze the fragility of structures. Based on the numerical simulation results, Equation (5) for the engineering demand parameter is determined through regression fitting. Subsequently, by substituting Equation (5) into Equations (6) and (7), the fragility of the tower-line system under combined ice and wind loads can be calculated [22].

$$\ln(EDP) = a\ln(IM_1) + b\ln(IM_2) + c \tag{5}$$

$$F[EDP \geq LS|IM] = \Phi\left(\frac{\ln(EDP) - \ln(LS)}{\beta_{EDP|IM}}\right) \tag{6}$$

$$\beta_{EDP|IM} = \sqrt{\frac{\sum_{i=1}^{n}[\ln EDP_i - (a\ln(IM_{1i}) + b\ln(IM_{2i}) + c)]^2}{n-2}} \tag{7}$$

where EDP is the engineering demand parameter; a, b, and c are the regression coefficients; IM_1 is the ice thickness; IM_2 is the wind speed; Φ represents standard normal distribution; LS is the limit performance indexes; $\beta_{EDP|IM}$ is the lognormal standard deviation of EDP.

3. Uncertain FEMs of Tower-Line Systems

In this paper, a 220 Kv transmission line with one tower and two span lines is employed as the research object. The total height of the transmission tower is 50.043 m, with a nominal height of 33.043 m, and the base size is 10 × 10 m. The main members of the tower are composed of Q345-type equilateral angle steel, and the diagonal and secondary members are composed of Q345-type and Q235-type equilateral angle steel. The employed tower is shown in Figure 2. The conductor and ground wire are 2-bundled JL/LB20A-630/45 and OPGW-105 optical cables, respectively, and the design parameters are shown in Table 1.

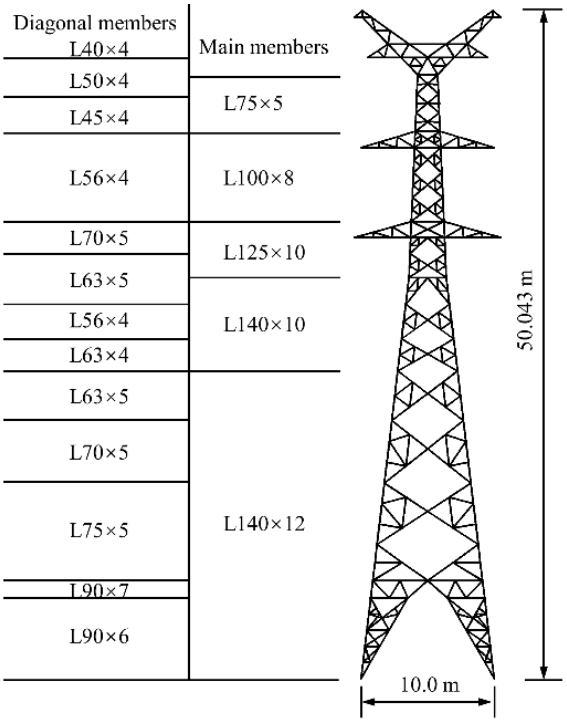

Figure 2. The size of the tower.

Table 1. Design parameters of conductors and ground wires.

Type	Diameter (mm)	Mass (kg/m)	Area (mm^2)	Elastic Modulus (MPa)
JL/LB20A-630/45	33.60	2.0072	666.55	65,000
OPGW-105	11.40	0.4170	68	132,000

During the design state of the structure, all model parameters are considered to be constant. However, in practical engineering cases, deviations from these designed values can occur during production, transportation, and installation processes, affecting material strength, geometric dimensions, and other structural parameters. Thus, the geometric size, material strength, boundary conditions, and other parameters of the whole tower-line system model are uncertain. Since the soil–structure interaction is not considered in this paper, the foot of the transmission tower is fixed. In addition, compared with the size of the tower, the span of the transmission line is larger, and the section size is smaller [40]. Therefore, the uncertainty of material parameters (yield strength, elastic modulus, and Poisson's ratio) and geometric dimensions (limb width and limb thickness of the angle steel) of the members in the tower are considered.

According to the Chinese code [41], for structural material strengths that conform to a lognormal distribution, the standard strength value is equivalent to the 0.05 quantile of the probability distribution, which is calculated using Equation (8). The standard values for the elastic modulus and Poisson's ratio of the material correspond to the 0.5 quantile of the probability distribution, which is the mean value. Table 2 presents the probability distribution of member material parameters. Regarding the uncertainty of geometric dimensions, existing research has demonstrated that the geometric dimensions of angle steel conform to a normal distribution, with the specific probability distribution as shown in Table 3 [40].

$$f_k = \mu_f \exp\left(-1.645\delta_f\right) \tag{8}$$

where f_k is the material strength standard value; μ_f is material strength standard value; δ_f is the variable coefficient of material strength.

Table 2. The probability distribution of member material parameters.

Uncertainty Parameters	μ_f	δ_f	Distribution
Elasticity modulus (GPa)	206	0.03	Lognormal distribution
Poisson's ratio	0.3	0.03	Lognormal distribution
Yield strength for Q235 (MPa)	263.7	0.07	Lognormal distribution
Yield strength for Q345 (MPa)	387.1	0.07	Lognormal distribution

Notes: μ_f denotes the material strength standard value; δ_f denotes the variable coefficient of material strength.

Table 3. The probability distribution of geometric dimensions.

Uncertainty Parameters	Average Value	δ_f	Distribution
Limb thickness	0.985	0.032	Normal distribution
Limb width	1.001	0.008	Normal distribution

Notes: δ_f denotes the variable coefficient of material strength.

After establishing the probability distribution of uncertainty parameters, the LHS method is employed to extract 30 groups of member parameters. Then, 30 uncertain FEMs (U1-U30) and 1 certain FEM (C1) of the transmission tower-line system are established by ANSYS (the version is ANSYS V19). The BEAM188 element is used to simulate the transmission tower, and the LINK10 element is used to simulate the transmission line [42]. The Bilinear isotropic hardening plasticity model is used to describe the constitutive model of the steel member [34]. The foot of the transmission tower and the two ends of the transmission lines are fixed.

It should be noted that the influence of initial defects introduced by the initial uniform mode method is considered in the subsequent analysis [34]. To ensure the accuracy of the calculation results, each member of the transmission tower is divided into three elements. Figures 3 and 4 show the sampling results of yield strength and elastic modulus of Q235-type steel and the FEM of transmission tower-line system, respectively. The specific uncertain material parameters of uncertain FEMs are listed in Appendix A.

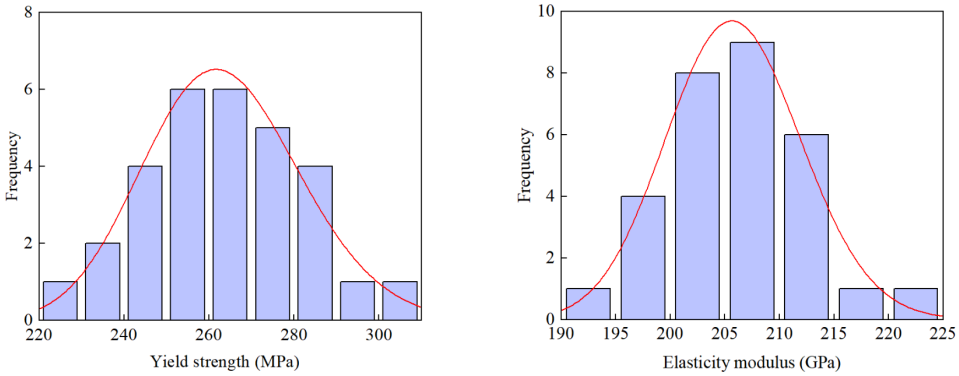

Figure 3. The sampling results: (**a**) samples of yield strength for Q235; (**b**) samples of elasticity modulus.

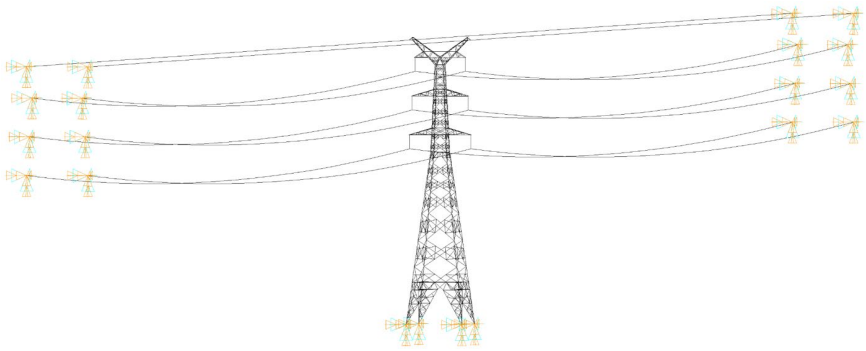

Figure 4. The FEM of transmission tower-line system.

4. Limit Performance Index

4.1. Pushover Analysis

To obtain the fragility of transmission lines, it is necessary to determine the limit performance index of transmission tower-line systems. Once the mechanical response of the transmission tower exceeds the limit performance index, the transmission line is considered to collapse. The tower top displacement of the transmission tower is adopted as the engineering demand parameter [35], and the maximum tower top displacement is defined as the limit performance index of the tower, which is determined through Pushover analysis under combined ice and wind loads.

To facilitate the calculation, the transmission tower is divided into 12 simulation sections from bottom to top. The observation points of the tower and the diagram of the simulation section are shown in Figure 5. According to the Chinese code [43,44], the ice loads and the static wind loads of the tower and the transmission line are calculated by the following formulas.

$$W_x = \alpha_x \cdot W_o \cdot \mu_z \cdot \mu_{sc} \cdot \beta_c \cdot d \cdot L_P \cdot B_1 \tag{9}$$

$$W_s = W_o \cdot \mu_z \cdot \mu_s \cdot B_2 \cdot A_s \cdot \beta_z \tag{10}$$

$$W_o = v_{10}^2/1600 \tag{11}$$

where W_x is the wind load perpendicular to the transmission line; W_s is the wind load on the tower; W_o is the basic wind pressure value at a height of 10 m; α_x is the uniformity

coefficient of wind pressure; μ_z is the coefficient of wind pressure variation with height; μ_{sc} and μ_s are the shape coefficients of the transmission line and the tower, respectively; L_P and d are the span and diameter of the transmission line, respectively; B_1 and B_2 are the wind load increase coefficient of the transmission line with accreted ice and the tower with accreted ice, respectively; v_{10} is the mean wind speed at a height of 10 m; β_c and β_z are the wind load adjustment coefficients of the transmission line and the tower, respectively.

$$q_1 = \pi b \alpha_1 \alpha_2 (d + b \alpha_1 \alpha_2) \gamma \cdot 10^{-6} \tag{12}$$

$$q_a = 0.6 b \alpha_2 \gamma \cdot 10^{-3} \tag{13}$$

where q_1 and q_a are ice load per unit length of the transmission line and the ice load per unit area of the transmission tower members, respectively; b is the ice thickness at a height of 10 m; α_1 is the ice thickness correction coefficient related to the diameter; α_2 is the height increasing coefficient of ice thickness; γ is the volumetric weight of ice.

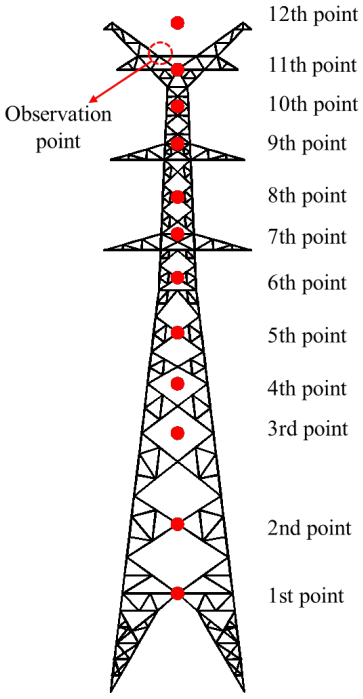

Figure 5. The diagram of the simulation section and the observation point.

In addition, since the unfavorable wind direction of the transmission tower is 90°, which is the vertical direction of the line, this direction is selected for wind vibration analysis. And, to consider the influence of the initial eccentricity of the structure caused by construction and other factors, the initial defects of the structure are introduced into the numerical model by using the uniform mode method before the analysis. More specific details of the uniform mode method can be found in Li et al. [9] and Fu et al. [34].

4.2. Sensitivity Analysis

Although the structural uncertainty parameters that need to be considered have been confirmed in Section 3, the influence of various uncertainty parameters on the mechanical response of structures has not yet been clarified. Therefore, the sensitivity analysis is performed to discuss the key parameters on the mechanical properties of structures. A series of additional FEMs of the transmission tower-line system are established, based on the structural uncertainty parameters extracted by the LHS method [45]. The difference from the above-established uncertainty model (U1-U30) is that only one parameter uncertainty is considered in each model of this series, and the remaining parameters are consistent with

those in the certain model C1. Subsequently, the influence of the parameters is analyzed in terms of the ultimate wind speed of the transmission line with different ice thicknesses.

The tornado diagrams with different ice thicknesses are given in Figure 6. The red line represents the ultimate wind speed of the C1 model, and the uncertainty parameters are arranged along the vertical axis from top to bottom, based on the degree of deviation of each from the results of the C1 model. Figure 6 indicates that the geometric dimensions of tower members, elasticity modulus, and the yield strength for Q345 have a significant effect on the ultimate wind speed of the transmission line with 5-mm ice thicknesses. As the ice thickness increases, the influence of geometric dimensions and yield strength of Q345 remain significant. The reason is that Q345-type equilateral angle steel is employed to manufacture the main members of towers and the diagonal members of the tower legs, which are the main bearing members of the tower. Similarly, when the section dimension changes, the bearing capacity and bending resistance of angle steel members also change. Therefore, the geometric dimensions of members and the yield strength for Q345 are the key parameters that affect the mechanical properties of the tower subjected to ice and wind loads in this paper. However, Q235-type equilateral angle steel serves primarily as the material for secondary members, which are mainly a constructional measure of the transmission tower, unlike the main load-bearing members. Thus, the yield strength for Q235 has a relatively minor influence on the ultimate wind speed of transmission lines under different ice thicknesses.

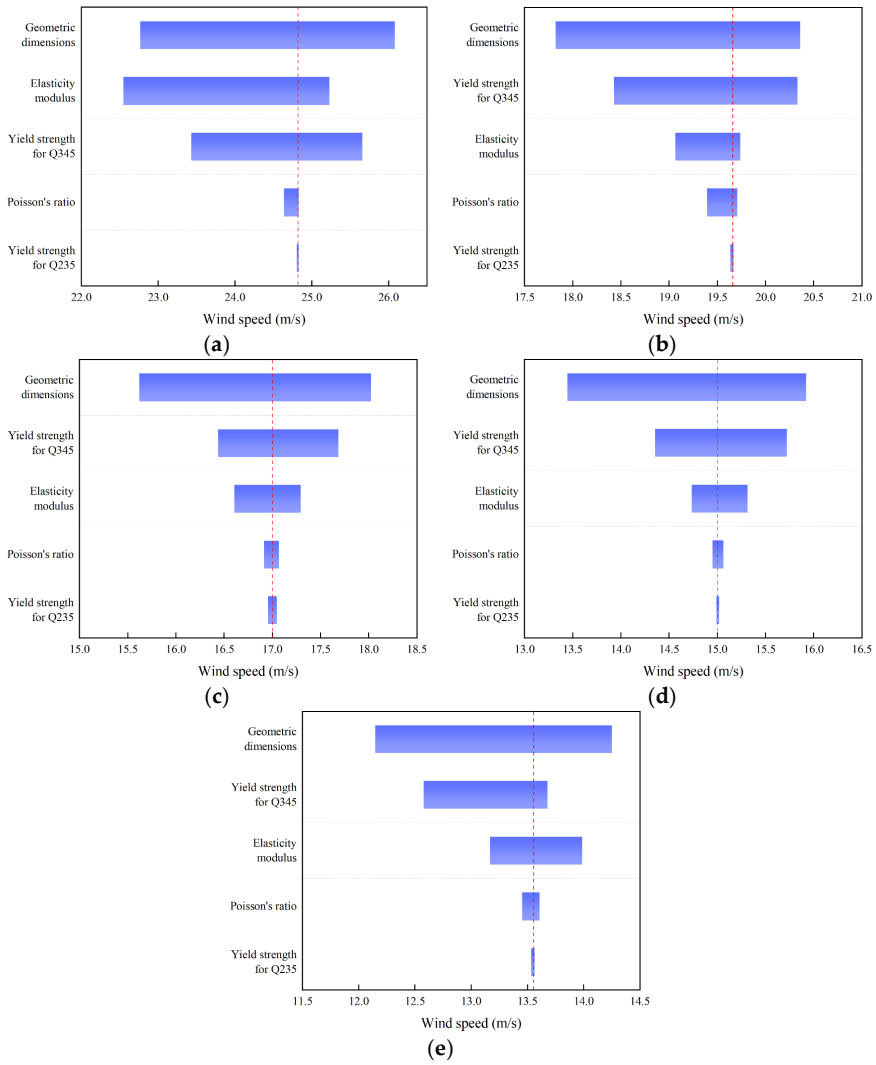

Figure 6. Tornado diagrams: (**a**) 5-mm ice thickness; (**b**) 10-mm ice thickness; (**c**) 15-mm ice thickness; (**d**) 20-mm ice thickness; (**e**) 25-mm ice thickness.

In summary, all the uncertain parameters selected have different degrees of influence on the mechanical property of the tower. Therefore, all structural uncertain parameters should be considered to more accurately evaluate the failure probability of transmission lines under combined ice and wind loads.

4.3. Determined Limit Performance Index

Wind load pushover analyses of 30 uncertain models (U1-U30) and 1 certain model (C1), each with varying ice thicknesses, are performed, and the displacement pushover curves of the tower top are obtained, as shown in Figure 7. Due to the uncertainty of material parameters and geometric dimensions, the maximum tower top displacement and ultimate wind speed of each model under different ice thicknesses are different, and with the increase in ice thickness, the ultimate wind speed gradually decreases. The pushover curve of the C1 model is basically located in the middle of the pushover curves of the U1-U30 models. Then, the limit performance index calculation formulas of different models are determined by linear regression fitting on maximum tower top displacement, as shown in Table 4. It can be seen that the fitting formulas have a strong correlation with the simulation results by calculating R^2. These formulas can be used to calculate the limit displacement of the tower top under different ice thicknesses. Once the displacement of the tower top exceeds this limit value, it indicates that the transmission tower fails. It should be noted that there is a large gap between the tower top displacement curves in Figure 7b, which occurs at a wind speed of 20 m/s. This is because, according to the Chinese code [43], the wind pressure non-uniformity factor and wind load adjustment factor used for calculating static wind loads differ significantly between wind speeds above and below 20 m/s. In contrast, due to the small ice thickness, this phenomenon did not occur in Figure 7a.

Table 4. The calculation formula of the limit performance index.

Case No.	The Calculation Formula	R^2	Case No.	The Calculation Formula	R^2
U1	$LS = -0.0056x + 0.4167$	0.9923	U16	$LS = -0.00596x + 0.4256$	0.9400
U2	$LS = -0.0051x + 0.3919$	0.9499	U17	$LS = -0.00602x + 0.4433$	0.9910
U3	$LS = -0.00584x + 0.433$	0.9075	U18	$LS = -0.00568x + 0.416$	0.9881
U4	$LS = -0.0052x + 0.4054$	0.9129	U19	$LS = -0.00564x + 0.4252$	0.9050
U5	$LS = -0.0055x + 0.3991$	0.9744	U20	$LS = -0.00638x + 0.4449$	0.9337
U6	$LS = -0.00638x + 0.4509$	0.9601	U21	$LS = -0.00498x + 0.3951$	0.9531
U7	$LS = -0.00538x + 0.3969$	0.9980	U22	$LS = -0.00556x + 0.3994$	0.9082
U8	$LS = -0.00542x + 0.4043$	0.9916	U23	$LS = -0.00598x + 0.4295$	0.9854
U9	$LS = -0.00596x + 0.4216$	0.9322	U24	$LS = -0.00546x + 0.4091$	0.9767
U10	$LS = -0.00616x + 0.4366$	0.9862	U25	$LS = -0.00598x + 0.4251$	0.9221
U11	$LS = -0.00598x + 0.4509$	0.9900	U26	$LS = -0.00592x + 0.4256$	0.9879
U12	$LS = -0.00616x + 0.433$	0.9571	U27	$LS = -0.00562x + 0.4245$	0.9779
U13	$LS = -0.00628x + 0.4436$	0.9817	U28	$LS = -0.00454x + 0.4069$	0.9973
U14	$LS = -0.00606x + 0.4373$	0.9679	U29	$LS = -0.006x + 0.4418$	0.9905
U15	$LS = -0.0058x + 0.3966$	0.9377	U30	$LS = -0.0068x + 0.4656$	0.9944
C1	$LS = -0.00562x + 0.4227$	0.9971			

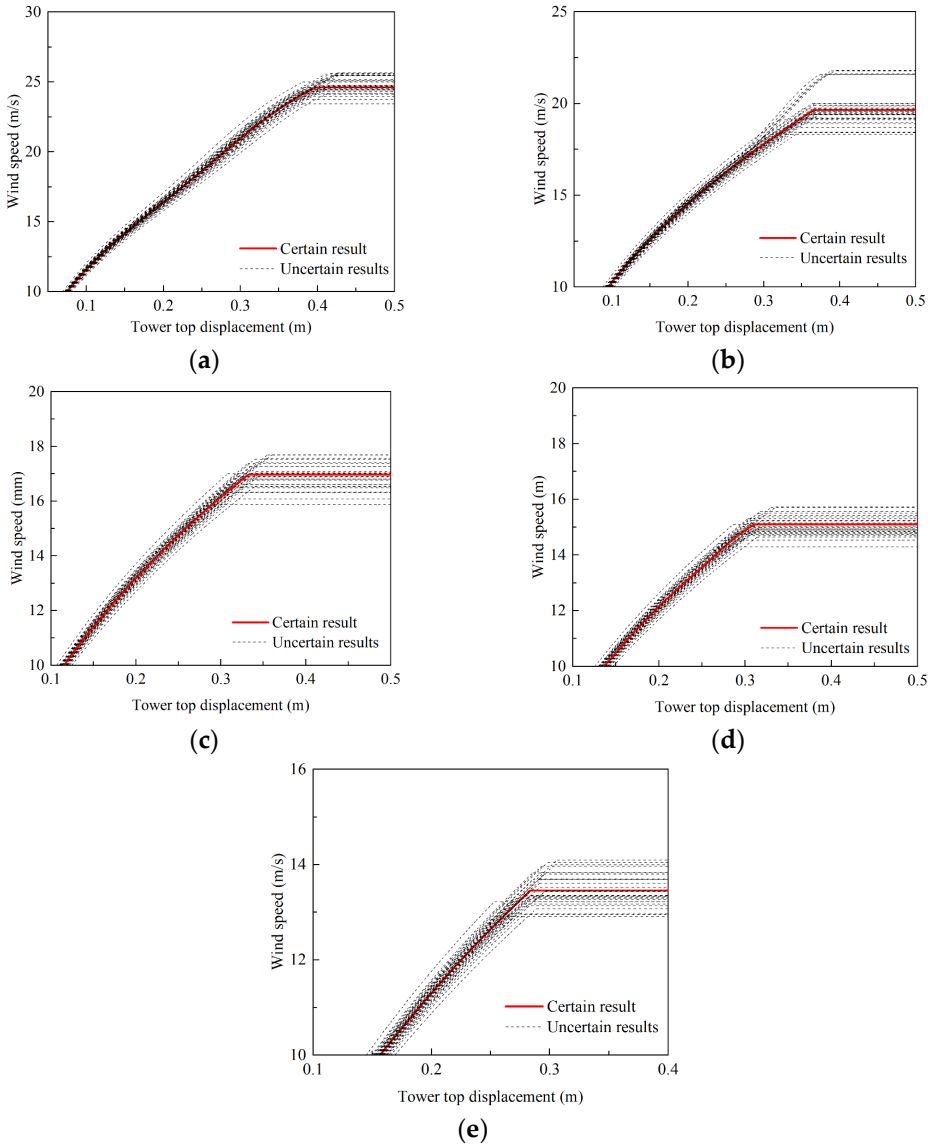

Figure 7. The pushover curve of the tower under different ice thicknesses: (**a**) 5-mm ice thickness; (**b**) 10-mm ice thickness; (**c**) 15-mm ice thickness; (**d**) 20-mm ice thickness; (**e**) 25-mm ice thickness.

5. Results

According to the Chinese code [46], the wind speeds corresponding to the design ice loads are 10 m/s (ice thickness less than 20 mm) and 15 m/s (ice thickness greater than 20 mm), respectively. The Pushover results indicate that the ultimate wind speed is 25 m/s (the ice thickness is 5mm), and the statistical maximum wind speed during icing events occurring between 1973 and 2020 is 24 m/s. Although the ultimate wind speed is 42.1 m/s when the ice load is not considered, the ultimate wind speed decreases while the ice thickness increases, as shown in Figure 8. In addition, the paper mainly focuses on the failure probability of the transmission lines during ice disasters, and it should be noted that the wind load cannot be ignored according to the Chinese code [46]. Therefore, the wind speed range of 0–24 m/s is selected for this study. Furthermore, to consider the influence of combined ice and wind loads on transmission lines in different ice regions, the ice thickness range is selected from 0 to 25 mm. Forty groups of combined ice and wind loads are randomly sampled to calculate the failure probability of the transmission tower-line system under combined ice and wind loads, as shown in Figure 9.

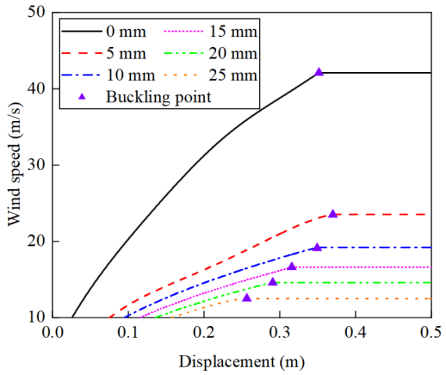

Figure 8. Load-displacement curves with different ice thicknesses.

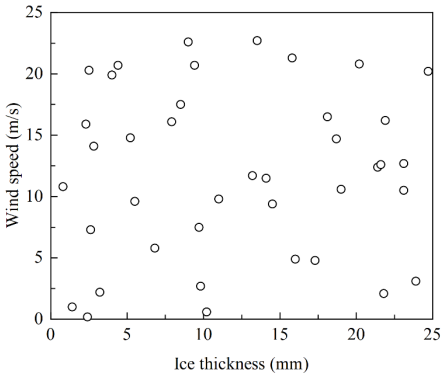

Figure 9. Random load samples.

5.1. Influence of Uncertain Parameters

To investigate the influence of structural uncertain parameters on the failure probability of transmission tower-line systems under combined ice and wind loads, this section performs static analysis for 30 uncertain models (U1-U30) and 1 certain model (C1), with the aim of obtaining the tower top displacements of different models under 40 load samples.

5.1.1. Fragility Analysis

The results from the 30 uncertain transmission tower-line system models (U1-U30) and the 1 certain model (C1) are substituted into Equation (5) for regression analysis, thereby determining the corresponding unknown parameters and establishing the calculation formula for *EDP*. Subsequently, the fragility functions for the 31 models are obtained using Equations (6) and (7), and the fragility surfaces under the collapse state of the transmission tower are drawn. Figure 10 presents the fragility surfaces of some models under combined ice and wind loads. It can be observed that significant differences exist in the fragility of transmission towers when considering the uncertainties of material parameters and geometric dimensions.

To more clearly compare the influence of uncertain parameters on the fragility of the tower-line system under combined ice and wind loads, Figure 11 presents the fragility curves under various ice thicknesses. It can be observed that the fragility curve of the C1 model is located in the middle of the fragility curves of U1-U30 models for all ice thicknesses. Table 5 compares the maximum and minimum exceedance probabilities of the transmission tower-line system under different ice thicknesses. When the ice thickness is 5 mm, the differences between the maximum and minimum exceedance probabilities at the three wind speeds are 0.07%, 1.65%, and 11.37%, respectively. It can be observed that the influence of uncertain parameters increases with the increasing wind speed with the same ice thickness when considering parameter uncertainties.

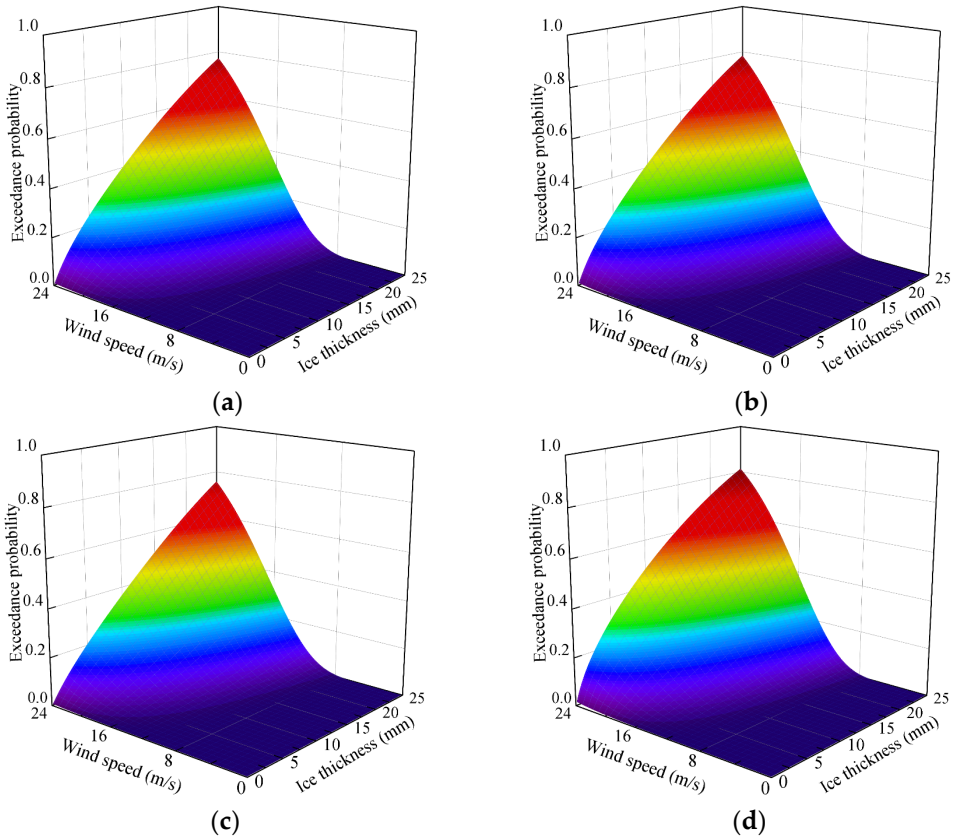

Figure 10. The fragility surfaces: (**a**) C1; (**b**) U1; (**c**) U6; (**d**) U21.

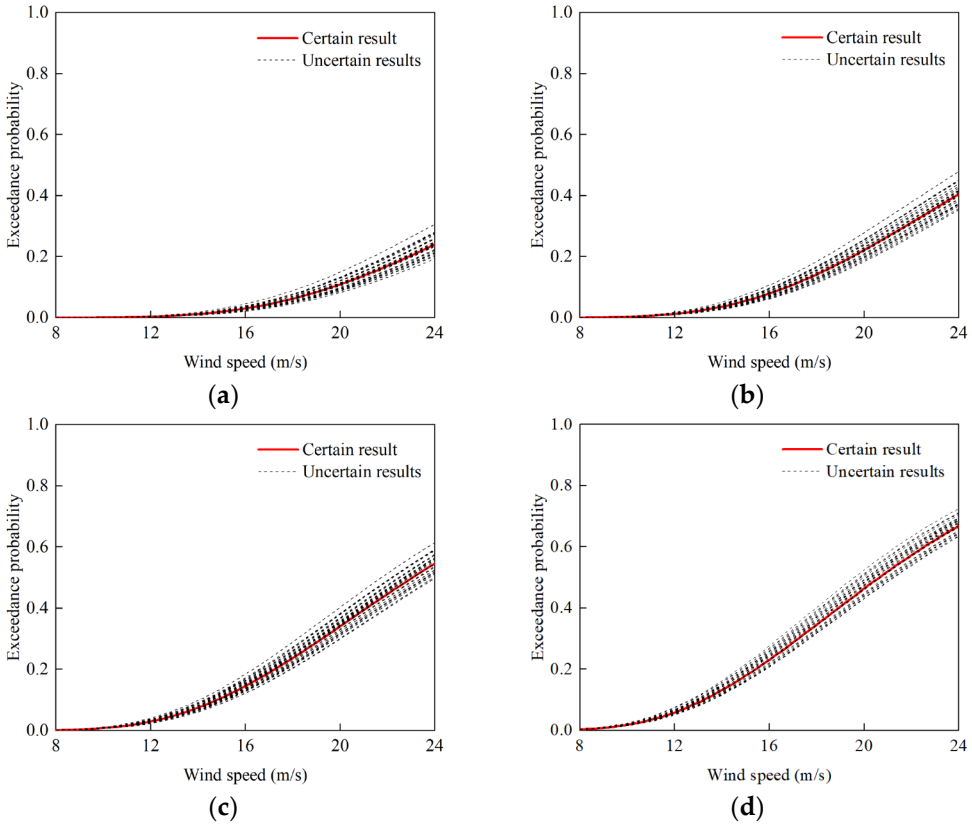

Figure 11. *Cont.*

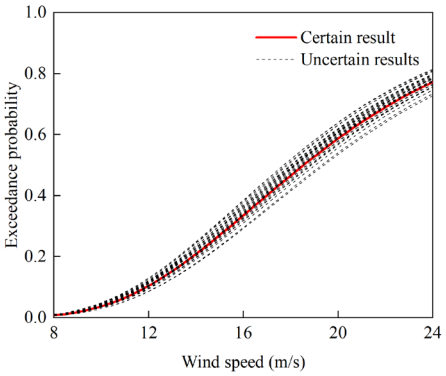

(**e**)

Figure 11. The fragility curves under different ice thicknesses: (**a**) 5-mm ice thickness; (**b**) 10-mm ice thickness; (**c**) 15-mm ice thickness; (**d**) 20-mm ice thickness; (**e**) 25-mm ice thickness.

Table 5. The exceedance probabilities.

Ice Thickness	Wind Speed 10 m/s		Wind Speed 15 m/s		Wind Speed 24 m/s	
	Maximum	Minimum	Maximum	Maximum	Minimum	Maximum
5 mm	0.11%	0.04%	2.98%	1.33%	30.69%	19.32%
10 mm	0.44%	0.19%	7.59%	4.2%	47.85%	35.34%
15 mm	1.13%	0.59%	13.77%	8.86%	61.36%	50.12%
20 mm	2.42%	1.59%	21.67%	15.98%	72.44%	63.34%
25 mm	4.68%	2.97%	31.33%	23.2%	81.4%	72.71%

5.1.2. Failure Probability Analysis

Combining the fragility function with the joint probability distribution of IT–WS and WS–WD, the failure probability density of transmission tower collapse under combined ice and wind loads is calculated by Equation (2). Figure 12 presents the failure probability density surfaces for the certain model C1 model and the uncertain model U21 model, which exhibit noticeable differences. Table 6 presents the cumulative failure probability of all models under combined ice and wind loads. Compared with the certain model, considering the parameter uncertainty, the cumulative failure probability of the tower-line system changes between 0 and 47%, and the ratio of the maximum to the minimum cumulative failure probability is approximately 1.84. This phenomenon indicates that uncertain parameters can lead to significant fluctuations in the failure probability of the tower-line system under combined ice and wind loads.

Table 6. The cumulative failure probability (unit: 10^{-5}).

Model Number	Probability	Model Number	Probability	Model Number	Probability
U1	2.0090	U11	1.4269	U21	2.6304
U2	2.3373	U12	1.7708	U22	2.4706
U3	1.5998	U13	1.7197	U23	1.7259
U4	2.3103	U14	1.6195	U24	2.1272
U5	2.3031	U15	2.1515	U25	2.0025
U6	1.5366	U16	1.7122	U26	2.0077
U7	2.4650	U17	1.7350	U27	1.8653
U8	2.0692	U18	2.1401	U28	1.7766
U9	2.0545	U19	2.2018	U29	1.8129
U10	1.8713	U20	1.6213	U30	1.4414
C1	1.8628				

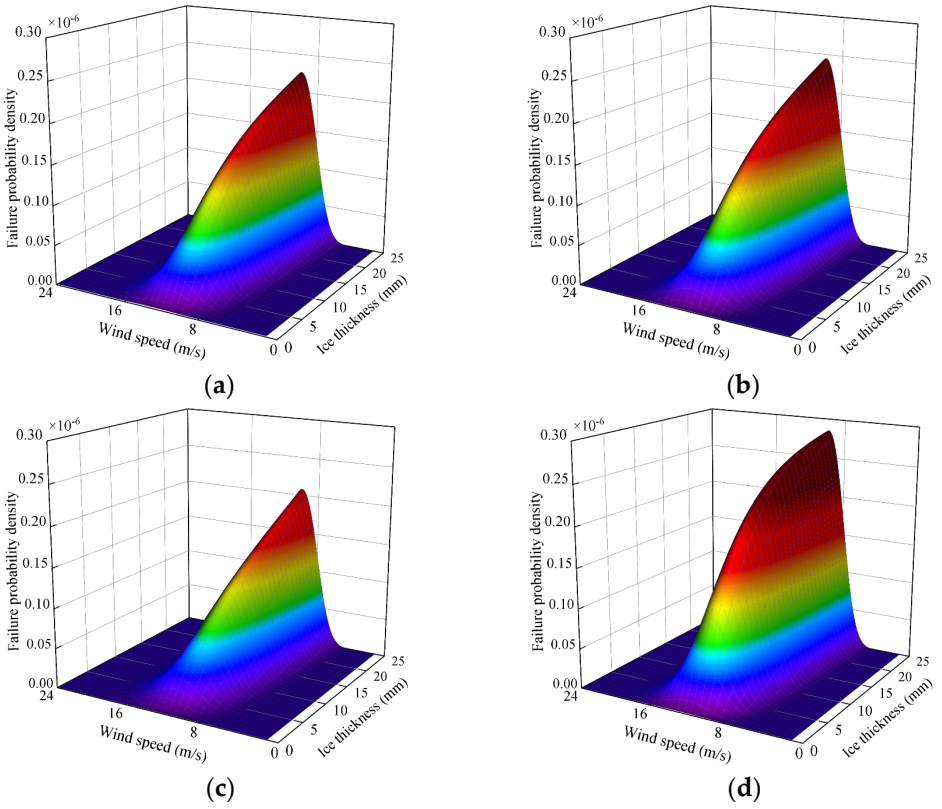

Figure 12. The failure probability density surfaces: (**a**) C1; (**b**) U1; (**c**) U6; (**d**) U21.

5.2. Influence of Wind Fluctuating Effect

To further investigate the failure probability of transmission lines under combined ice and wind loads, this section considers the fluctuating effects of wind loads and conducts a dynamic analysis of transmission tower-line systems considering uncertainty. The fluctuating wind speed is simulated by the harmonic superposition method with the Davenport spectrum. The duration is 300 s, and the cut-off frequency is 5 Hz [47]. In addition, for the static analysis, the wind load is calculated by Equations (9)–(11). To ensure the reasonability of the comparison results, the turbulence intensity of 0.14 specified in the Chinese code is adopted. The wind speed at point 11, and the comparison between simulated and target spectra, are shown in Figure 13. The mean wind speed of each section is calculated by exponential law formula [42]:

$$v(z) = v_{10} \cdot \left(\frac{z}{10}\right)^{\alpha} \tag{14}$$

where $v(z)$ is the mean wind speed at a height of z m; v_{10} is the mean wind speed at a height of 10 m; α is the ground roughness index, which is 0.15 for the landform category B.

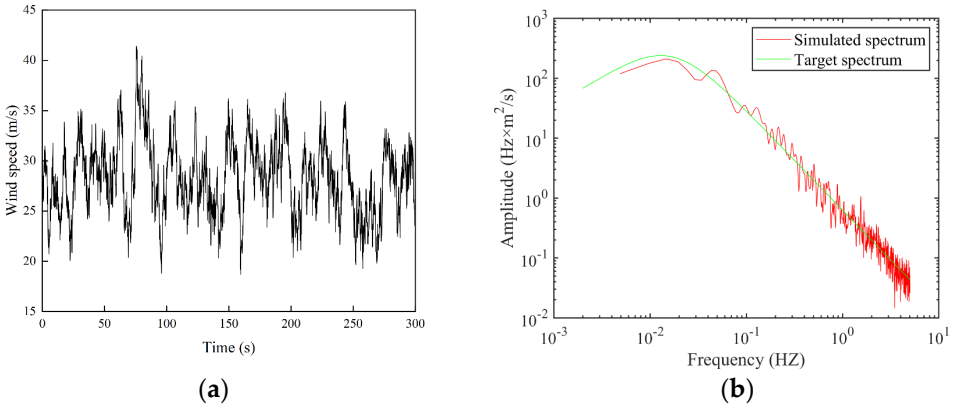

Figure 13. The wind at point 11 ($v_{10} = 20\text{m/s}$): (**a**) wind speed; (**b**) wind spectra comparison.

Then, the total wind speed of each section is obtained by superimposing the mean wind speed and the fluctuating wind speed, and then converted into wind load using Equation (15) [30,34,47]:

$$F_i(t) = \mu_s \rho A_i V_i^2 / 2 \quad (15)$$

where μ_s is the shape coefficient of the structure; A_i is the windward area; V_i is the total wind speed; ρ is the air density.

5.2.1. Fragility Analysis

The nonlinear static and dynamic analyses of 30 groups of uncertain models under combined ice and wind loads are carried out, and the corresponding fragility surfaces are obtained, as shown in Figure 14. Figure 15 presents the fragility curves of the tower-line system under different ice thicknesses. It can be seen that the fragility surface considering the fluctuating effect is located above the fragility surface of the static analysis. The maximum exceedance probabilities of static analysis and dynamic analysis are 77.58% and 88.23%, respectively, and the difference reaches 12.06%, which indicates that the fragility of the tower-line system increases significantly after considering the fluctuating effect.

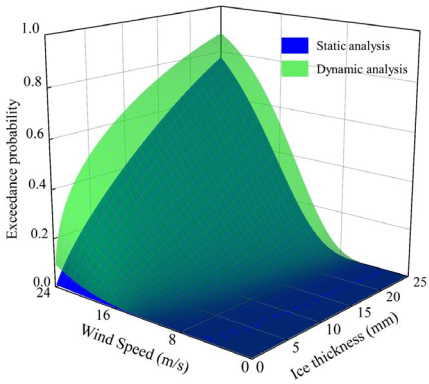

Figure 14. The comparison of fragility surfaces.

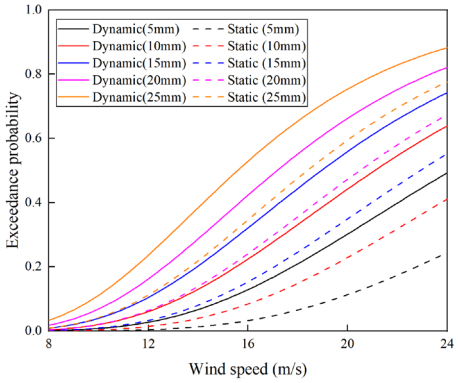

Figure 15. The comparison of fragility curves.

Table 7 compares the maximum and minimum exceedance probabilities of the transmission tower-line system under both static and dynamic loads. When the ice thickness is 5 mm, the differences between the maximum and minimum exceedance probabilities at the three wind speeds are 0.70%, 7.39%, and 24.83%, respectively. And under the same wind speed, the difference gradually increases with the increase in ice thickness. Additionally, the difference between the exceedance probabilities obtained from the static and the dynamic analyses is more evident than the influence of uncertainty parameters. This phenomenon indicates that the fluctuating effect has a more significant effect on the fragility of the tower-line system.

Table 7. The comparison of exceedance probabilities.

Ice Thickness	Wind Speed 10 m/s		Wind Speed 15 m/s		Wind Speed 24 m/s	
	Dynamic	Static	Dynamic	Static	Dynamic	Static
5 mm	0.77%	0.07%	9.51%	2.12%	49.26%	24.43%
10 mm	2.02%	0.33%	17.46%	5.91%	63.88%	41.12%
15 mm	3.95%	0.91%	26.03%	11.37%	74.19%	55.2%
20 mm	6.86%	2.06%	35.5%	18.72%	82.11%	67.35%
25 mm	11.14%	4.15%	45.81%	28.11%	88.23%	77.58%

5.2.2. Failure Probability Analysis

By substituting the fragility functions derived from the static and dynamic analyses into Equations (2) and (3), respectively, the corresponding failure probability densities are calculated and presented in Figure 16. Within the loading range selected in this paper, the shapes of the failure probability density surfaces obtained from the static and dynamic analyses exhibit significant differences. Specifically, due to the fluctuating effect of the wind, the failure probability peaks at an ice thickness of 10.125 mm in the dynamic analysis, whereas in the static analysis the peak failure probability density aligns with an ice thickness of 25 mm. The corresponding wind speeds for these maximum failure probability densities are 10.08 m/s and 9.96 m/s, respectively. It can be observed that in the dynamic analysis, the failure probability density corresponding to an ice thickness of 25 mm is lower than that of 10.125 mm. The reason for this phenomenon is that when ice thickness increases from 10.125 mm to 25 mm, although the exceedance probability increases from 0.0217 to 0.1156, the joint probability density of ice and wind decreases from 4.193×10^{-5} to 5.774×10^{-6}. In this case, the joint probability distribution of ice and wind exerts a more significant influence than the fragility, resulting in a downward trend in the failure probability density. This phenomenon indicates that, after considering the fluctuating effect of wind, even smaller ice loads can potentially lead to the failure of the transmission tower-line system.

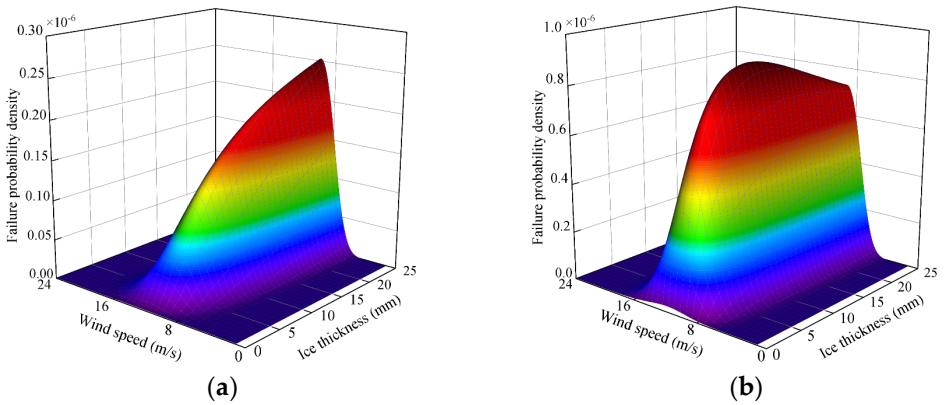

Figure 16. The failure probability density surfaces: (**a**) static analysis; (**b**) dynamic analysis.

Table 8 presents the cumulative failure probabilities of the tower-line system obtained from both static and dynamic analyses. After considering the fluctuating effect of wind, the cumulative failure probability of the tower-line system increases by 4.7 times. Furthermore, for the scenario examined in this paper, accounting for the joint probability distribution of wind speed and direction results in a notable reduction in the failure probability of the transmission line under combined ice and wind loads. This phenomenon underscores the significance of considering joint distribution, as neglecting it can yield inaccurate failure probability estimates for transmission tower-line systems.

Table 8. The cumulative failure probabilities.

The Joint Probability of the WS–WD	Dynamic Analysis	Static Analysis
Without	0.15	0.0321
With	0.0099	0.0021

6. Conclusions

In this paper, the method for failure probability of the transmission line considering uncertainty under combined ice and wind loads has been presented. It is based on the joint probability distribution models of ice thickness–wind speed and wind speed–wind direction and the fragility analysis of uncertain structures. The specific case is used to explain the detailed process for this method, and the influence of structural parameter uncertainty and wind fluctuating effect on failure probability is studied.

The failure probabilities of 30 uncertain models and 1 certain model were calculated. Compared to the influence of uncertain parameters, the influence of fluctuating wind on the failure probability of the tower-line system is more significant. After considering the fluctuating effect of wind, the smaller ice loads can potentially lead to the failure of the tower-line system, and the cumulative failure probability increases by 4.7 times compared with the static analysis.

Subsequently, the structural uncertainty leads to significant fluctuations in the failure probability of tower-line systems under combined ice and wind loads, whose fluctuating range is from 0.12% to 47.34%. Under the same ice thickness, the influence of parameter uncertainty increases with the increase in wind speed.

In addition, through sensitivity analysis, all uncertain parameters have an effect on the mechanical properties of the tower subjected to ice and wind loads, and the influences of the geometric dimensions of tower members and the yield strength for main members are the most significant. Notice that, ignoring the joint probability distribution of ice and wind loads would lead to an incorrect estimation of the failure probability for the tower-line system.

The failure probability analysis method for transmission line considering uncertainty employed in this paper is not only applicable to transmission tower-line systems but also to other types of structure. For areas with missing accreted ice data, this method can be linked to the Jones prediction model to establish a joint probability distribution model of ice and wind loads (see, e.g., Li et al. [39]), and thereby the failure probability can be calculated. Furthermore, it can also analyze the failure probabilities of structures located in other regions subjected to various coupled loads such as combined wind and seismic loads.

Author Contributions: Conceptualization, J.L. and J.Z.; methodology, J.L., C.Z., J.Z., X.Z. and W.W.; software, J.L., C.Z., J.Z., X.Z. and W.W.; validation, J.Z. and X.Z.; investigation, J.L. and J.Z.; writing—original draft preparation, J.L., C.Z. and J.Z.; writing—review and editing, J.L. and C.Z.; visualization, C.Z. and W.W.; supervision, J.Z. and X.Z.; project administration, J.L., J.Z. and X.Z. All authors have read and agreed to the published version of the manuscript.

Funding: This research was funded by the Fundamental Research Funds for the Central Universities (Grant No. N2301012).

Institutional Review Board Statement: Not applicable.

Informed Consent Statement: Not applicable.

Data Availability Statement: The original contributions presented in the study are included in the article; further inquiries can be directed to the corresponding author.

Conflicts of Interest: Author Jian Zhang was employed by the company Northeast Electric Power Design Institute Co., Ltd. Author Xuesheng Zhang was employed by the company Beijing Urban Construction Group Co., Ltd. The remaining authors declare that the research was conducted in the absence of any commercial or financial relationships that could be construed as potential conflicts of interest.

Appendix A

Table A1. The specific uncertain material parameters of uncertain FEMs.

Case No.	Elasticity Modulus (GPa)	Poisson's Ratio	Yield Strength for Q235 (MPa)	Yield Strength for Q345 (MPa)
U1	205.47	0.2962	270.17	376.18
U2	209.76	0.2931	275.48	361.69
U3	213.20	0.3057	265.31	419.00
U4	199.18	0.2906	302.10	365.39
U5	210.26	0.3172	238.70	357.80
U6	207.40	0.2822	276.80	425.90
U7	204.50	0.2961	242.80	331.20
U8	212.00	0.3088	236.36	370.28
U9	203.50	0.3106	262.89	382.70
U10	200.10	0.3005	255.14	388.46
U11	209.10	0.3071	256.21	437.70
U12	208.16	0.2989	272.08	405.42
U13	202.49	0.3012	280.55	397.01
U14	210.86	0.2922	250.43	408.01
U15	222.36	0.2976	273.58	351.95
U16	215.70	0.2869	252.20	392.30
U17	198.55	0.2894	284.50	402.70
U18	201.63	0.2955	281.56	369.62
U19	191.12	0.3019	245.38	381.60
U20	207.99	0.3116	264.38	414.06
U21	195.01	0.3030	260.45	347.52
U22	204.08	0.3038	259.84	353.47
U23	211.36	0.3049	289.68	394.99
U24	206.56	0.3078	246.88	373.20
U25	202.79	0.3027	248.29	384.97
U26	201.36	0.2995	226.84	377.74
U27	205.16	0.2950	295.89	387.62
U28	214.47	0.3144	268.30	410.42
U29	196.94	0.2936	257.27	399.30
U30	205.99	0.2983	266.93	442.66

References

1. Jiang, X.; Zhu, M.; Dong, L.; Hu, Q.; Zhang, Z.; Hu, J. Site Experimental Study on Suspension-Tension Arrangement for Preventing Transmission Lines from Icing Tripping. *Int. J. Elec. Power.* **2020**, *119*, 105935. [CrossRef]
2. Wang, J.; Fu, C.; Chen, Y.; Rao, H.; Xu, S.; Yu, T.; Li, L. Research and Application of DC De-Icing Technology in China Southern Power Grid. *IEEE T. Power Deliver.* **2012**, *27*, 1234–1242. [CrossRef]
3. Yang, F.; Yang, J.; Zhang, Z.; Zhang, H.; Xing, H. Analysis on the Dynamic Responses of a Prototype Line from Iced Broken Conductors. *Eng. Fail. Anal.* **2014**, *39*, 108–123. [CrossRef]
4. Jiang, X.; Xiang, Z.; Zhang, Z.; Hu, J.; Hu, Q.; Shu, L. Predictive Model for Equivalent Ice Thickness Load on Overhead Transmission Lines Based on Measured Insulator String Deviations. *IEEE T. Power Deliver.* **2014**, *29*, 1659–1665. [CrossRef]
5. Zhang, J.; Makkonen, L.; He, Q. A 2D Numerical Study on the Effect of Conductor Shape on Icing Collision Efficiency. *Cold Reg. Sci. Technol.* **2017**, *143*, 52–58. [CrossRef]
6. Zhang, J.; He, Q.; Makkonen, L. A Novel Water Droplet Size Parameter for Calculation of Icing on Power Lines. *Cold. Reg. Sci. Technol.* **2018**, *149*, 65–70. [CrossRef]
7. Yang, L.; Chen, Y.; Hao, Y.; Li, L.; Li, H.; Huang, Z. Detection Method for Equivalent Ice Thickness of 500-kV Overhead Lines Based on Axial Tension Measurement and Its Application. *IEEE T. Instrum. Meas.* **2023**, *72*, 9001611. [CrossRef]
8. Li, J.; Wang, B.; Sun, J.; Wang, S.; Zhang, X.; Fu, X. Collapse Analysis of a Transmission Tower-Line System Induced by Ice Shedding. *Front. Phys.* **2021**, *9*, 712161. [CrossRef]
9. Li, J.; Li, H.; Fu, X. Stability and Dynamic Analyses of Transmission Tower-Line Systems Subjected to Conductor Breaking. *Int. J. Struct. Stab. Dyn.* **2017**, *6*, 1771013. [CrossRef]
10. Lehner, P.; Krejsa, M.; Parenica, P.; Krivy, V.; Brozovsky, J. Fatigue Damage Analysis of a Riveted Steel Overhead Crane Support Truss. *Int. J. Fatigue* **2019**, *128*, 105190. [CrossRef]
11. Brozovsky, J.; Krejsa, M.; Lehner, P.; Parenica, P.; Seitl, S. Reliability Analysis of Bridge Details from High-Strength Steel with Use of DOProC Approach: Challenges and Research Directions. *AIP Conf. Proc.* **2023**, *2950*, 020032. [CrossRef]

12. Ferrari, R.; Cocchetti, G.; Rizzi, E. Evolutive and Kinematic Limit Analysis Algorithms for Large-Scale 3D Truss-Frame Structures: Comparison Application to Historic Iron Bridge Arch. *Int. J. Comp. Meth.* **2020**, *17*, 1940020. [CrossRef]
13. Ferrari, R.; Cocchetti, G.; Rizzi, E. Effective Iterative Algorithm for the Limit Analysis of Truss-Frame Structures by a Kinematic Approach. *Comput. Struct.* **2018**, *197*, 28–41. [CrossRef]
14. Ferrari, R.; Cocchetti, G.; Rizzi, E. Reference Structural Investigation on a 19th-Century Arch Iron Bridge Loyal to Design-Stage Conditions. *Int. J. Archit. Herit.* **2020**, *14*, 1425–1455. [CrossRef]
15. Cocchetti, G.; Cornaggia, A.; Ferrari, R.; Rizzi, E. Consistent Complementarity Problem Formulation for the Mechanical Modellisation of Spatial Cable–Rib Structures. In *Italian Workshop on Shell and Spatial Structures*; Lecture Notes in Civil Engineering; Gabriele, S., Manuello Bertetto, A., Marmo, F., Micheletti, A., Eds.; Springer: Cham, Switzerland, 2023; Volume 437. [CrossRef]
16. Cocchetti, G.; Liu, R.; Cornaggia, A.; Ferrari, R.; Rizzi, E. Elastic–Plastic Optimisation of a Cable–Rib Satellite Antenna. In *Direct Methods for Limit State of Materials and Structures: Advanced Computational Algorithms and Material Modelling*; Lecture Notes in Applied and Computational Mechanics; Garcea, G., Weichert, D., Eds.; Springer: Cham, Switzerland, 2023; Volume 101. [CrossRef]
17. Pan, H.; Li, C.; Tian, L. Seismic Fragility Analysis of Transmission Towers Considering Effects of Soil-Structure Interaction and Depth-Varying Ground Motion Inputs. *Bull. Earthq. Eng.* **2021**, *19*, 4311–4337. [CrossRef]
18. Ma, L.; Khazaali, M.; Bocchini, P. Component-Based Fragility Analysis of Transmission Towers Subjected to Hurricane Wind Load. *Eng. Struct.* **2021**, *242*, 112586. [CrossRef]
19. Zhu, C.; Yang, Q.; Huang, G.; Zhang, X.; Wang, D. Fragility Analysis and Wind Directionality-Based Failure Probability Evaluation of Transmission Tower under Strong Winds. *J. Wind. Eng. Ind. Aerod.* **2024**, *246*, 105668. [CrossRef]
20. Tian, L.; Pan, H.; Ma, R. Probabilistic Seismic Demand Model and Fragility Analysis of Transmission Tower Subjected to Near-Field Ground Motions. *J. Constr. Steel. Res.* **2019**, *156*, 266–275. [CrossRef]
21. Dikshit, S.; Alipour, A. A Moment-Matching Method for Fragility Analysis of Transmission Towers under Straight Line Winds. *Reliab. Eng. Syst. Safe.* **2023**, *236*, 109241. [CrossRef]
22. Fu, X.; Li, H.; Li, G. Fragility Analysis and Estimation of Collapse Status for Transmission Tower Subjected to Wind and Rain Loads. *Struct. Saf.* **2016**, *58*, 1–10. [CrossRef]
23. Li, C.; Pan, H.; Tian, L.; Bi, W. Lifetime Multi-Hazard Fragility Analysis of Transmission Towers under Earthquake and Wind Considering Wind-Induced Fatigue Effect. *Struct. Saf.* **2022**, *99*, 102266. [CrossRef]
24. Xiao, M.; Zhou, W.; Bitsuamlak, G.; Hong, H. Fragility of Transmission Tower-Line System Subjected to Concurrent Wind and Ice Accretion. *J. Constr. Steel. Res.* **2024**, *222*, 108925. [CrossRef]
25. Mahmoudi, A.; Nasrollahzadeh, K.; Jafari, M. Probabilistic Failure Analysis of 400 kV Transmission Tower-Line System Subjected to Wind and Ice Hazards. *Wind. Struct.* **2021**, *33*, 251–264. [CrossRef]
26. Yang, H.; Huang, L.; He, C.; Yi, D. Probabilistic Prediction of Transmission Line Fault Resulted from Disaster of Ice Storm. *Power Syst. Technol.* **2012**, *36*, 213–218. [CrossRef]
27. Yang, H.; Chung, C.; Zhao, J.; Dong, Z. A Probability Model of Ice Storm Damages to Transmission Facilities. *IEEE Trans. Power Deliver.* **2013**, *28*, 557–565. [CrossRef]
28. Yang, H.; Xu, W.; Zhao, J.; Wang, D.; Dong, Z. Predicting the Probability of Ice Storm Damages to Electricity Transmission Facilities Based on ELM and Copula Function. *Neurocomputing* **2011**, *74*, 2573–2581. [CrossRef]
29. Li, J.; Wang, W.; Fu, X.; Jiang, W.; Dong, Z. Failure Probability Analysis of Transmission Towers under Ice-Wind Interaction. *J. Vib. Shock* **2024**, *43*, 136–146. [CrossRef]
30. Liang, S.; Zou, L.; Wang, D.; Cao, H. Investigation on wind tunnel tests of a full aeroelastic model of electrical transmission tower-line system. *Eng. Struct.* **2015**, *85*, 63–72. [CrossRef]
31. Fu, Z.; Tian, L.; Luo, X.; Pan, H.; Liu, J.; Liu, C. Study on the Influence of Structural and Ground Motion Uncertainties on the Failure Mechanism of Transmission Towers. *Earthq. Struct.* **2024**, *26*, 311–326. [CrossRef]
32. Pan, H.; Tian, L.; Fu, X.; Li, H. Sensitivities of the Seismic Response and Fragility Estimate of a Transmission Tower to Structural and Ground Motion Uncertainties. *J. Constr. Steel Res.* **2020**, *167*, 105941. [CrossRef]
33. Fu, X.; Li, H.; Tian, L.; Wang, J.; Cheng, H. Fragility Analysis of Transmission Line Subjected to Wind Loading. *J. Perform. Constr. Fac.* **2019**, *33*, 04019044. [CrossRef]
34. Fu, X.; Li, H. Uncertainty Analysis of the Strength Capacity and Failure Path for a Transmission Tower under a Wind Load. *J. Wind. Eng. Ind. Aerod.* **2018**, *173*, 147–155. [CrossRef]
35. Wang, J.; Li, H.; Fu, X.; Dong, Z.; Sun, Z. Wind Fragility Assessment and Sensitivity Analysis for a Transmission Tower-Line System. *J. Wind. Eng. Ind. Aerod.* **2022**, *231*, 105233. [CrossRef]
36. Tian, L.; Liu, K. Uncertainty Analysis of the Dynamic Responses of a Transmission Tower-Line System Subjected to Cable Rupture. *J. Wind. Eng. Ind. Aerod.* **2021**, *34*, 04020088. [CrossRef]
37. Fu, Z.; Tian, L.; Liu, J. Seismic Response and Collapse Analysis of a Transmission Tower-Line System Considering Uncertainty Factors. *J. Constr. Steel. Res.* **2011**, *189*, 107094. [CrossRef]
38. Ma, Y.; Dai, Q.; Pang, W. Reliability Assessment of Electrical Grids Subjected to Wind Hazards and Ice Accretion with Concurrent Wind. *J. Struct. Eng.* **2020**, *146*, 04020134. [CrossRef]
39. Li, J.; Zuo, Y.; Wang, L.; Dong, Z. Fragility Analysis of a Transmission Tower-Line System Subjected to Wind and Ice Loads Considering Fatigue Damage. *Int. J. Struct. Stab. Dyn.* **2024**, 2550074. [CrossRef]

40. Fu, X.; Li, H.; Li, G.; Dong, Z. Fragility Analysis of a Transmission Tower under Combined Wind and Rain Loads. *J. Wind. Eng. Ind. Aerod.* **2020**, *199*, 104098. [CrossRef]
41. *GB 50068-2018*; Ministry of Housing and Urban-Rural Development of the People's Republic of China. Unified Standard for Reliability Design of Building Structures. China Architecture & Building Press: Beijing, China, 2018.
42. Liu, C.; Wang, T.; Tang, Z.; Li, Z. Time-Varying Wind-Resistance Global Reliability Analysis of In-Service Transmission Tower Using High-Order Moments-Based Improved Maximum Entropy Method. *Appl. Sci.* **2023**, *13*, 4245. [CrossRef]
43. *DL/T 5154-2012*; National Energy Administration. Technical Code for the Design of Tower and Pole Structures of Overhead Transmission Line. China Planning Press: Beijing, China, 2012.
44. *GB50135-2019*; Ministry of Housing and Urban-Rural Development of the People's Republic of China. Standard for Design of High-Rising Structures. China Planning Press: Beijing, China, 2019.
45. Helton, J.; Davis, F. Latin Hypercube Sampling and the Propagation of Uncertainty in Analyses of Complex Systems. *Reliab. Eng. Syst. Saf.* **2003**, *81*, 23–69. [CrossRef]
46. *DL/T 5440-2020*; National Energy Administration. Technical Specification for the Design of Overhead Transmission Line in Medium and Heavy Icing Area. China Planning Press: Beijing, China, 2020.
47. Fu, X.; Li, H.; Yang, Y. Calculation of Rain Load Based on Single Raindrop Impinging Experiment and Applications. *J. Wind. Eng. Ind. Aerod.* **2015**, *147*, 85–94. [CrossRef]